Available online at www.sciencedirect.com
SCIENCE DIRECT
Earth and Planetary Science Letters 244 (2006) 431–443
EPSL
www.elsevier.com/locate/epsl

Silicon isotope fractionation during nutrient utilization in the North Pacific

Ben C. Reynolds [a,*], M. Frank [b], A.N. Halliday [c]

[a] IGMR, Departement Erdwissenschaften, Sonneggstrasse 5, ETH Zentrum NO, CH-8092 Zürich, Switzerland
[b] IfM-GEOMAR, Leibniz Institute for Marine Sciences at the University of Kiel, Wischhofstrasse 1-3, 24148 Kiel, Germany
[c] Department of Earth Sciences, Parks Road, Oxford, OX1 3PR, UK

Received 3 November 2005; received in revised form 17 January 2006; accepted 2 February 2006

Editor: H. Elderfield

Abstract

The distribution of silicon in the North Pacific is controlled by the utilization of silicic acid by diatoms, a process that fractionates silicon (Si) isotopic compositions. Silicon isotope variations are presented for six water column profiles from the surface mixed layer down to the deep waters of the North Pacific Ocean. Although the observed Si isotopic variations display an apparently simple inverse relationship with dissolved nutrient concentrations, in fact they reflect mixing of surface waters undergoing active Si isotope fractionation and deep-waters with more uniform concentrations and isotope compositions. Samples from the surface of the subtropical gyre have the lowest dissolved Si concentrations and heaviest Si isotope compositions of marine waters measured thus far. Fractionation in the surface waters follows a typical Rayleigh-type distillation curve for a 'closed' surface water reservoir resulting from stratification of the surface layer in the subarctic region. In contrast, an 'open' system prevails within the subtropical gyre where there is significant recycling of silicic acid in the upper water column and lateral transport of silicon within surface currents. For deep waters, the Si isotope composition distinguishes between the northern North Pacific Deep Water (NPDW) and the southerly-derived bottom water. The relatively light Si isotope compositions measured from waters within the subarctic gyre provides evidence for isolation of the nutrient pool in the North Pacific.

Keywords: silicon isotopes; North Pacific; nutrients

1. Introduction

Silicic acid is an important nutrient in the surface oceans as it is required for the growth of diatoms, radiolarians, and silicoflagellates. In high nutrient and coastal regions, diatoms can account for over half of the primary production in, and export of carbon from the surface oceans [1–3]. As biogenic silica production is dependent on the supply of dissolved silicic acid to the euphotic zone, silicon (Si) is an important limiting element. Diatoms dominate the biogeochemical cycling of Si, and they strongly influence the biogeochemical cycles of the other macro-nutrients, such as nitrogen (N) and phosphorus (P). In the high latitude areas of the oceans, light limitation allows for nutrient concentrations to build up over winter [4], and iron limitation results in year round high nitrate but low chlorophyll concentrations in the surface waters (HNLC) [5]. The

* Corresponding author. Tel.: +41 44 632 6869; fax: +41 44 632 1179.
E-mail address: reynolds@erdw.ethz.ch (B.C. Reynolds).

0012-821X/$ - see front matter © 2006 Elsevier B.V. All rights reserved.
doi:10.1016/j.epsl.2006.02.002

abundant nutrients in these HNLC regions are then partially utilized during spring blooms, with diatom productivity dominating the large phytoplankton community [6]. In the North Pacific, artificial iron (Fe) fertilisation experiments also lead to higher diatom productivity indicating Fe limitation of diatom growth within the subarctic gyre [6,7]. High dust supply from Asia may provide Fe to the surface waters in the western North Pacific, thus reducing Fe limitation and distinguishing between the nutrient regimes in the western subarctic gyre (WSG) and the eastern Alaska Gyre (AG). For these two HNLC areas seasonal cyclicity is stronger in the WSG where utilization of macronutrients is increased during the summer and where Si : Nitrate ratios are higher, indicative of higher diatom production [4,8]. Within the AG, the migration of eddies has been shown to strongly influence nutrient dynamics and the supply of Fe from coastal regions into the surface waters of the gyre [9]. The subarctic gyre of the North Pacific is thus a good place to test the role of dust fertilization on the phytoplankton productivity as dust deposition decreases dramatically from the WSG to the AG.

In order to assess changes in marine productivity over time for modelling global climate change and for understanding global biogeochemical cycles, better constraints on the utilisation of nutrients in the surface oceans are required. Changes in the marine Si cycle and diatom paleoproductivity may be assessed from Si stable isotopes because they fractionate during biogenic utilization. During the uptake of silicic acid and mineralization of diatoms, there is a preferential incorporation of the lighter isotopes into biogenic silica [10]. This results in the enrichment of heavy isotopes in seawater and a geological record of silicic acid utilization and availability in the isotope composition of sedimentary biogenic opal [11]. To date, there has only been a very limited number of records of Si isotope variations in seawater to assess the marine distribution of Si isotopes and validate its use as a proxy for nutrient utilization [12–14]. Published open marine Si isotope studies have focused on the Southern Ocean, with only one deep-water profile measured in the Pacific Ocean and two profiles in the Atlantic [14]. Clearly, more data are required to establish the broad applicability of the Si isotope proxy and to reliably exploit its potential in paleoceanography [15].

Initial modelling of the distribution of Si isotopes in the world oceans has been carried out by integration of a biogeochemical ocean circulation model [16], but differences between measured and modelled surface silicic acid concentrations indicate that the model does not capture the real nutrient utilization in high latitudes [16]. For deep water, the model predicts much smaller differences between the Atlantic and Pacific than observed. Obviously the biogeochemical models require further data to better constrain the dissolution of biogenic silica.

Technical advances now allow Si isotopes to be analysed relatively quickly with minimal sample preparation, such that their global distribution can be established at relatively high resolution. We have investigated the dissolved Si isotope composition in the North Pacific in order to better understand the biogeochemical cycle of Si. The North Pacific was surveyed in 2002 as part of the

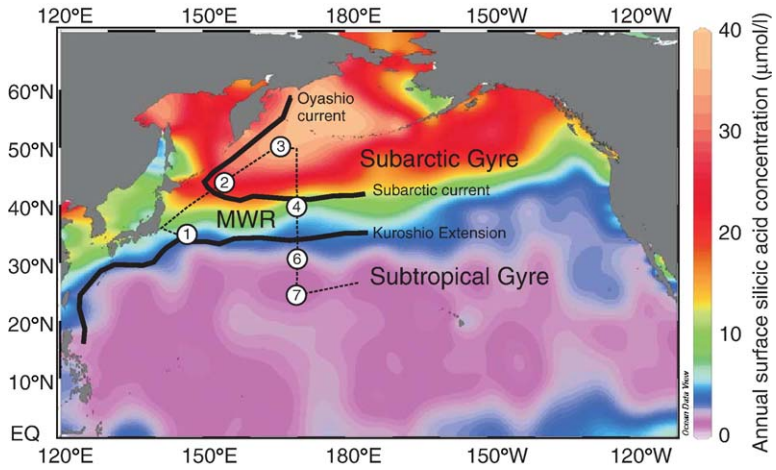

Fig. 1. Map showing the location of the vertical stations (circles with Station numbers) analysed along the cruise track (dotted line) for the 2002 IOC Contaminant Baseline Survey in the western Pacific Ocean. Shading denote annual average Si concentrations in the water column given by the World Ocean Atlas 2001 (WOA01) Data [42] compiled for Ocean Data View [43].

Table 1
Seawater nutrient concentrations and δ^{30}Si data for samples from 2002 IOC Contaminant Baseline Survey in the western Pacific Ocean, collected in May 2002 [39]

Station no.	Lat. °N	Long. °E	Water depth (m)	Nutrient conc. [17]				Volume used (ml)	δ^{30}Si (‰)	$2\sigma_{SD}$ (±)	$2\sigma_{SEM}$ (±)
				NO_3 (μM)	PO_4 (μM)	SiO_2 (μM)	Si (ppm)				
1	34.5	147.0	100	1.6	0.1	3.6	0.1	50	2.43	0.12	0.08
1	34.5	147.0	600	29.5	1.8	77.6	2.2	14	1.14	0.09	0.08
1	34.5	147.0	1500	46.8	3.2	151.7	4.3	2	0.61	0.10	0.08
2	44	155	10	16.4	1.7	38.3	1.1	14	1.42	0.06	0.08
2	44	155	100	23.1	1.9	43.5	1.2	14	1.16	0.05	0.08
2	44	155	600	45.0	3.3	148.9	4.2	2	0.85	0.07	0.08
2	44	155	1200	44.3	3.3	172.1	4.8	2	0.51	0.06	0.08
2	44	155	4000	35.0	2.7	158.3	4.4	2	0.83	0.15	0.08
2	44	155	5000	32.6	2.7	158.6	4.4	2	0.71	0.10	0.08
3	50	167	10	22.4	1.5	42.4	1.2	14	1.23	0.17	0.08
3	50	167	100	24.5	1.8	44.7	1.3	14	1.14	0.06	0.08
3	50	167	600	44.4	3.3	142.2	4.0	2	0.72	0.14	0.08
3	50	167	1500	42.3	3.2	174.2	4.9	2	0.52	0.11	0.08
4	39.4	170.6	10	5.8	0.4	15.8	0.4	14	1.31	0.28	0.08
4	39.4	170.6	100	14.5	1.1	20.8	0.6	14	1.46	0.22	0.06
4	39.4	170.6	600	43.0	3.2	107.6	3.0	2	0.72	0.12	0.06
4	39.4	170.6	1500	47.7	3.5	176.2	4.9	2	0.74	0.06	0.06
4	39.4	170.6	1500	Duplicate				2	0.67	0.06	0.06
6	30.5	170.6	100	3.5	0.2	3.9	0.1	50	2.15	0.17	0.08
6	30.5	170.6	600	25.7	2.2	53.5	1.5	14	1.37	0.15	0.08
6	30.5	170.6	1500	45.6	3.6	166.3	4.7	2	0.64	0.01	0.08
7	24.3	170.3	50	0.0	0.1	0.6	0.02	100	3.15	0.13	0.08
7	24.3	170.3	100	3.5	0.2	4.3	0.1	50	2.55	0.14	0.08
7	24.3	170.3	300	9.1	0.9	6.6	0.2	50	1.40	0.12	0.06
7	24.3	170.3	600	29.0	2.0	50.3	1.4	14	1.32	0.03	0.08
7	24.3	170.3	900	42.7	3.2	119.6	3.4	2	1.31	0.08	0.08
7	24.3	170.3	1200	43.2	3.3	140.2	3.9	2	1.09	0.08	0.08
7	24.3	170.3	2000	39.5	2.8	167.1	4.7	2	1.06	0.16	0.07
7	24.3	170.3	2000	Duplicate				2	1.17	0.23	0.11
7	24.3	170.3	3500	36.6	2.5	161.6	4.5	2	1.18	0.03	0.08
7	24.3	170.3	4000	36.2	2.3	160.3	4.5	2	0.86	0.08	0.06
7	24.3	170.3	5000	34.5	2.3	149.2	4.2	2	0.85	0.15	0.07
7	24.3	170.3	5700	35.1	2.3	145.7	4.1	2	1.05	0.07	0.06

Seawater profiles for nitrate, phosphate and silicic acid concentrations from [17]. A systematic offset of 17% lower Si concentrations were measured for samples in our laboratory. The volume used denotes the volume of seawater processed using $Mg(OH)_2$ precipitation for Si isotope analyses. The analytical error on the δ^{30}Si value is given as the 2 standard deviation of the mean from 5 or 7 duplicate standard bracket analyses, and the 95% confidence limit of the standard error of the mean, taking into account of a generally greater standard deviation of the long-term reproducibility of our in-house standard (±0.135‰). Station numbers refer to vertical profile stations at positions shown in Fig. 1, and occupied on the cruise on the 6th, 12th, 15th, 16th, 20th and 23rd of May 2002 for Stations 1, 2 (KNOT), 3, 4, 6 and 7, respectively.

Intergovernmental Oceanographic Commission (IOC) Contaminant Baseline Survey encompassing the subtropical and subarctic gyre of the western North Pacific [17]. Surface nutrient concentrations in this area vary from typical nutrient depleted surface waters to nutrient replete waters within the low salinity surface waters of the subarctic gyre. The phytoplankton assemblages are dominated by diatoms, which makes this area ideal for studying variations in Si isotopes as a function of nutrient utilisation. Below the surface waters, a salinity minimum across the North Pacific subtropical gyre marks the intrusion of North Pacific Intermediate Water (NPIW) [18], which is derived from mixing of fresher waters from the Sea of Okhotsk and thermocline waters from the subtropical gyre at about 40°N [19]. There are two other subsurface water masses of importance; bottom waters derived from the southern ocean, generally termed Lower Circumpolar Water or Antarctic Bottom Water (AABW), and an overlying deep water mass characterised by high Si concentrations referred to as North Pacific Deep Water [20]. In this paper we aim to explore the variations in Si isotope compositions between different water masses and during fractionation in the surface waters caused by biological utilisation.

2. Samples and methods

All samples were collected aboard the R/V Melville between May 1 and June 3, 2002, along a cruise track from Japan into the HNLC region of the North Pacific and then south along 170°E as shown in Fig. 1. Subsurface waters were collected using a rosette with Niskin bottles, which were then sub-sampled aboard ship through 0.45 μm Millipore cellulose filters into pre-cleaned polypropylene bottles (pre-cleaned with 2 M HCl and trace amounts of HF for several weeks). Samples were acidified to pH ~2 with HCl (~0.1% v/v conc HCl), as the samples were collected for determination of HF concentrations. Samples were transported back to ETH Zürich and stored in cool dark conditions for over 1 year, before an aliquot was taken for Si isotope analyses. Dissolved nutrient concentrations for phosphate, nitrogen (as NO_2 and NO_3) and silicic acid were determined on frozen samples returned to Hawaii using conventional colorimetric reactions [17], and shown in Table 1. The high purity acids and onboard handling of samples did not introduce any significant Si blank.

Silicon was separated and purified using a modified magnesium co-precipitation technique [13,21,22] followed by ion-exchange chromatography. Silicic acid semi-quantitatively co-precipitates with $Mg(OH)_2$. However, contrary to previous studies [13,22,23], we observed that this method can significantly fractionate Si isotopes, with low recovery resulting in enrichment of the lighter Si isotopes. To avoid isotope fractionation and ensure high yields a two-step co-precipitation is required. As our determination method for stable Si isotope variations consumes between 10 and 30 nmol of Si and in order to duplicate analyses and check chemical purity we separated between 0.1 and 1 μmol of Si (see Table 1), which required only 2 ml of seawater for concentrations above 100 μM Si. Only a brief synopsis of the chemical separation and mass-spectrometric techniques is presented here because a full description of these methods is beyond the scope of this paper and will be published separately [24].

The $Mg(OH)_2$ was precipitated directly from the acidified seawater samples at a pH of ~9.7 by the addition of 2% by volume of 1 M NaOH. Sample were shaken and left for 1 h, then centrifuged. The supernate was removed and an addition of 1% by volume of 1 M NaOH was added to form more $Mg(OH)_2$ precipitate. Again samples were shaken, left for 1 h and centrifuged. The supernate was analysed for Si concentration using a molybdate-blue spectrophotometric method to check for complete removal of Si. Measured concentrations that were above the detection limit of 3 ppb showed that the two-stage co-precipitation process efficiently removes more than 97% of the dissolved Si from the seawater. The precipitates were dissolved in 6 M HCl. Using this method of pre-concentration, it was possible to concentrate Si by at least a factor of 50. Separation of Si from other ions was achieved quantitatively using a cation-exchange resin (BioRad AG50W-X12), on which cations bind, but silicic acid does not, using water as the elute [24] and ensuring 100% yields. Samples were typically loaded on a 1.8 ml resin bed in 200 μl of 0.1 M HCl, and washed through with 5 ml water. All solutions were checked for complete removal of Mg and other trace cations. The separated Si fraction was diluted directly in teflon vials to a concentration of 600 ppb (21 μM) for introduction into the mass spectrometer. Unfortunately this chemical purification does not separate Si from other uncharged elements including P and Ge, although these elements are much less abundant in seawater and do not interfere with our Si isotope analyses by ICP-MS.

The Si isotope analyses were carried out on the unique Nu1700 high-resolution MC-ICP-MS (at ETH Zürich) in dry plasma mode using a standard-sample-standard bracketing technique. The 600 ppb Si solutions were introduced into the plasma via a Nu Instruments DSN desolvator equipped with a PFA nebuliser and using a 60–80 μl/min uptake rate. Concentrations of Si and HCl were matched between sample and standard with typical concentrations of 600 ppb Si in 0.01 M HCl. No hydrofluoric acid was used as this acid strongly alters the mass-bias stability, dramatically increases blank contributions, and results in loss of SiF_4 during desolvation of the aerosol, which introduces Si isotope fractionation. Background levels are reduced to 10^{-13} A for $^{28}Si^{+}$ by the use of a semi-demountable alumina-injector torch. The Nu1700 uniquely provides true mass-resolution from an adjustable source defining slit and individual adjustable collector slits widths, which allow the complete resolution of the three Si ion beams from all polyatomic isobaric interferences including $^{14}N^{16}O^{+}$, $^{28}SiH^{+}$, $^{14}N_2^{+}$ and $^{12}C^{16}O^{+}$. The three Si ion beams were collected simultaneously on Faraday collectors, with typical intensities of 6×10^{-11} A for $^{28}Si^{+}$. Analyses consisted of 36 × 10 s integrations and a 3 min wash cycle between samples and standards [24]. All results given are calculated in ‰ deviations from the international Si standard NBS28. The long-term reproducibility is better than 0.14‰ δ^{30}Si (2 standard deviations of the mean) [25]. Samples were measured at least 5 times, which resulted in a 95% confidence level below 0.08‰ δ^{30}Si, although 2 standard error of the mean for the sample duplicates were typically below this confidence level.

3. Results

The six water column profiles from the North Pacific are from three distinct hydrographic settings (Fig. 1); the subarctic gyre, the subtropical gyre, and a mixed water region (MWR) between the Subarctic and Kuroshio Extension Currents. For all stations Si concentrations increase rapidly from surface waters (<45 μmol Si) to about 1000 m depth (>130 μmol Si), as shown in Fig. 2 and Table 1. The measured δ^{30}Si values for these six profiles range from +0.5‰ to +3.2‰, and decrease from the surface waters to the deep waters (Fig. 2 and Table 1).

In the subarctic gyre, Stations 2 and 3 have relatively elevated Si concentrations in their surface mixed water layer of about 40 μM (Fig. 2d–f), and δ^{30}Si values between +1.1‰ and +1.4‰. The salinity distribution appears to show a remnant of the winter mixed layer at a depth of about 100 m in both stations. Sampling took place during the progressive seasonal stratification of this region with a shallower summer mixed layer occurring at Station 2, but no stratification at Station 3 [17]. Maximum surface chlorophyll concentrations were recorded south of these locations, but elevated chlorophyll concentrations (Chl *a*) in the upper 50 m indicate active diatom growth and the beginning of the spring bloom [17]. There is no NPIW in the subarctic gyre, and nutrient concentrations in the water column remain higher than in the subtropical gyre down to depths of 800 m for PO_4 and 2000 m for SiO_4. For the deeper samples (Station 2 only), the δ^{30}Si values are relatively low and only amount to +0.7‰ to +0.8‰.

For the subtropical gyre, Stations 6 and 7 have strong depletion of nutrients in the surface waters (Fig. 2a–c),

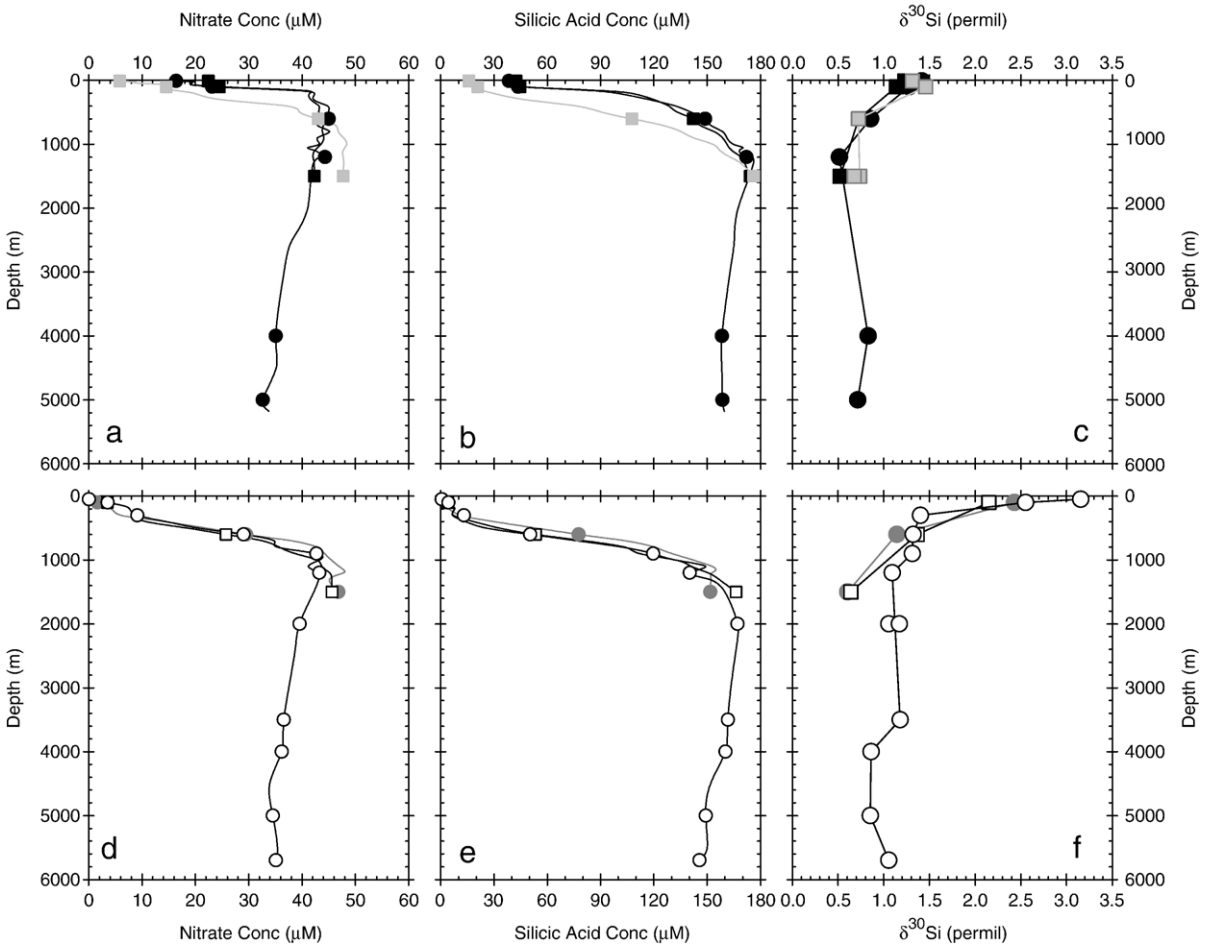

Fig. 2. Seawater profiles for nitrate concentrations (a and d), silicic acid concentrations (b and e) from [17] and sampled δ^{30}Si values (c and f) for subarctic regions (a–c) and subtropical (d–f). See Table 1 for more details. Symbols: gray circles = Station 1, black circles = Station 2, black squares = Station 3, gray squares = Station 4, black open squares = Station 6, and black open circles = Station 7. Error bars are within the size of the symbols.

below the detection limits of 0.05 μM PO_4 and 0.72 μM SiO_2. Si concentrations rapidly increase at all stations between 300 and 900 m depth, with a maximum concentration of 170 μM at about 2000 m followed by slightly decreasing concentrations (~10%) towards the bottom of the water column, where AABW prevails. The shallowest sample (50 m at Station 7) is from just below the surface mixed layer and has the highest so far recorded marine δ^{30}Si values: +3.2‰. At a concentration of only 0.6 μM, this concentration is an order of magnitude lower than any previously recorded seawater sample for which the Si isotope compositions has been determined. North Pacific Intermediate Water (NPIW) occupies the water column in the depth range of 300 to 900 m, and the measured δ^{30}Si values are uniform at +1.4±0.1‰. Below the NPIW, the δ^{30}Si values in the water column decrease steadily with depth until about 1500 m, where δ^{30}Si values of +0.8‰ and +0.6‰ are reached at Stations 7 and 6, respectively.

There are also two Mixed Water profiles (Stations 1 and 4), where active mixing of the surface waters was observed [17]. Station 4 is relatively close to the subarctic gyre and has a surface water Si concentration of 16–18 μM, whilst Station 1 is close to the subtropical gyre and has surface water nutrient concentrations below the limit of detection (Fig. 2). Nutrient and sampling profiles for these two stations did not extend below 1500 m. In terms of Si isotopes, the two profiles also reflect their hydrographic positions, with Station 4 being similar to subarctic Station 2 and Station 1 being similar to subtropical Station 6 (see Figs. 1 and 2). Vigorous eddy mixing, with pronounced salinity minimum layers accompanied by oxygen maxima, occur at Station 1 down to depths of 500 and 700 m [17].

4. Discussion

Previous measurements of the dissolved Si isotope composition of seawater have focused mainly on the Southern Ocean [12–14], where surface δ^{30}Si values vary from +1.7‰ to +3.1‰ [12,13] and deeper water (>800 m) δ^{30}Si values vary from +1.0‰ to +1.5‰ [13,14]. Initial results from the Atlantic and Pacific Ocean showed that the least positive seawater δ^{30}Si values were found in the central North Pacific (at 2000 m) [14], as δ^{30}Si values decrease along the thermohaline convection of deepwater from the Atlantic to the North Pacific via the Southern Ocean. These previous results are confirmed here, with low δ^{30}Si values recorded in the North Pacific at a depth >600 m. High δ^{30}Si values (>+2.0‰) have previously only been observed in surface waters of the Southern Ocean during active Si utilization. The high δ^{30}Si values reported here are from surface waters with very low Si concentrations, <5 μmol (140 ppb Si). The high δ^{30}Si values (>+2.0‰) reflect efficient preferential removal of lighter isotopes from the seawater by siliceous diatoms as they form biogenic silica [10]. To routinely investigate the Si isotope fractionation at such low concentrations, we developed new analytical techniques for the separation and purification of Si that enable analyses from only 60 nmol of Si in order to evaluate the use of δ^{30}Si as a proxy for nutrient utilization in the world's surface oceans.

4.1. Modeling Si isotope fractionation

The removal of Si from the surface waters and the Si isotope fractionation can be described by two simple models assuming either 'open' or 'closed' system behaviour. In an 'open' system a dynamic equilibrium is reached with a continuous supply of nutrients (assuming steady state conditions), whilst in a 'closed' system there is no further supply of nutrients and fractionation occurs along a Rayleigh-type distillation curve. These two models can be described approximately by the following equations:

$$\text{OPEN} \quad (\delta^{30}\mathrm{Si})_{\mathrm{W}} = (\delta^{30}\mathrm{Si})_{\mathrm{initial}} - \varepsilon \times (1-f) \tag{1}$$

where f is the enrichment factor, the relative depletion of dissolved Si concentrations, as a fraction of the initial concentration ($[\mathrm{Si(OH)_4}]_{\mathrm{W}}/[\mathrm{Si(OH)_4}]_{\mathrm{initial}}$), and ε is the fractionation factor between the dissolved and particulate phase.

$$\text{CLOSED} \quad (\delta^{30}\mathrm{Si})_{\mathrm{W}} = (\delta^{30}\mathrm{Si})_{\mathrm{initial}} + \varepsilon \times (1\mathrm{n}\ f)$$

or

$$(\delta^{30}\mathrm{Si})_{\mathrm{W}} = (\delta^{30}\mathrm{Si})_{\mathrm{initial}} + \varepsilon \times \ln[\mathrm{Si(OH)_4}]_{\mathrm{W}} - \varepsilon \times \ln[\mathrm{Si(OH)_4}]_{\mathrm{initial}} \tag{2}$$

Both models assume a constant fractionation factor, ε. For the oceans, this factor is the biological Si isotope fractionation induced by diatom growth, as they preferentially incorporate lighter Si isotopes into their opaline frustules from the ambient waters. Initial experimental work found ε was about −1‰ and independent of species and temperature (in the range 12–22 °C) [10], but further culture work is needed to expand the temperature range and to further investigate potential vital effects. A study of Si isotope compositions in surface waters of the Southern Ocean estimated the in situ ε [12], which was found to be significantly higher than previous estimates [10,14]. Differences between the biogenic silica and ambient waters ranged

between estimates of ε=−1.9‰ using either open-system behaviour and ε=−1.1‰ for closed-system behaviour. The closed-system model did not fit the data for the filtered biogenic silica, but this could be due to either contamination by lithogenic silica fragments (clays), especially south of the Southern Antarctic Circumpolar Current Front, or underestimation of the initial Si concentrations used to calculate the enrichment factor (f). (As discussed later, clay or dust contamination of Si isotope compositions is unlikely.) Later estimates of in situ ε, using a closed system model for individual depth profiles across the Polar Front of the Southern Ocean, ("a multi-box approach" [13]) were in agreement with ε=−1‰ [10]. The discrepancy between estimates of ε primarily arises from the ambiguous estimation of the initial conditions (both the concentration and initial Si isotope composition). A more complete study of the oceanic distribution of silicon isotopes, using general circulation models (GCMs), has shown that the relationship between the silicic acid concentration and its δ^{30}Si value is not the simple distillation curve expected if surface waters behave as closed systems [16].

For all the data from the North Pacific, there is a clear relationship between nutrient concentrations and the measured Si isotope compositions, so to a first-order δ^{30}Si values reflect nutrient levels in the oceans. When plotting the logarithmic concentrations against δ^{30}Si values (Fig. 3) all data fit a linear regression with R^2=0.99, 0.98 and 0.89 for ln[Si(OH)$_4$], ln[Nitrates], and ln[PO$_4$], respectively. Following Eq. (2), the good correlations could be taken to imply that the Si isotope distribution does behave like a simple system with variations related to the utilization of nutrients. The data plotted, however, include samples from below the euphotic zone, where there is no active biological fractionation of Si isotopes. The gradient of the relationship between δ^{30}Si values and ln[Si(OH)$_4$] would imply an average fractionation factor (ε) of only −0.4‰. This value is much lower than previous estimates [12–14], because the observed relationship is not a fractionation line, but rather the result of mixing between different fractionated Si pools. The estimated Si concentrations and δ^{30}Si distribution using GCMs [16] also suggests that the δ^{30}Si distribution is best explained by mixing of different water masses. The modelled δ^{30}Si distribution reflects a progressive increase across the surface oceans from the high and low latitudes into the subtropical gyres, with underlying layers reflecting a mixing of the highly fractionated surface waters into a uniform deep water. The active fractionation by diatoms occurs in the surface waters

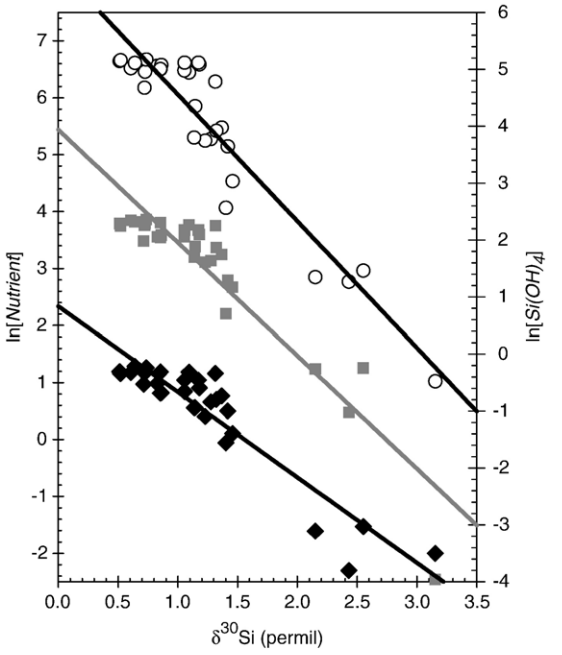

Fig. 3. Variations in seawater δ^{30}Si with nutrient concentrations in μM, plotted as ln[Phosphate] in black diamonds (R^2=0.89), ln[Nitrate] in gray squares (R^2=0.98), and ln[Si(OH)$_4$] in open circles with right axis (R^2=0.99). Data are from all stations in the North Pacific, but excludes one sample from 100 m water depth at Station 4. The lowest nitrate concentration (50 m depth at Station 7) is below the detection limit of 0.18 μM.

that are fed by intermediate waters, not usually deep-waters, such that deep-water concentrations and isotope compositions cannot be taken as initial conditions in the calculation of fractionation factors. The low apparent fractionation factor of −0.4‰ is simply a consequence of mixing between highly fractionated surface waters, intermediate waters and Si-rich deep-waters.

4.2. Surface water Si isotope fractionation

The biological utilization of Si by diatoms only occurs in the surface waters as the algae require light for photosynthesis, hence all marine Si isotope variations are ultimately derived from surface water productivity, if variations of the Si isotope composition of the continental Si supply can be excluded. The dissolution of sinking biogenic silica originating from the surface waters impart their Si isotope composition into the intermediate and deep waters. The distinction of these two regimes where Si is either actively removed from seawater or added via the dissolution of sinking particles can be easily achieved by plotting the δ^{30}Si values against nutrient concentrations, either Si, N or P, as shown in Fig. 4. There are 4 samples of seawater with

low nutrient concentrations where biological activity has actively removed most of the available nutrients. Excluding these 4 nutrient-depleted waters, the nutrient replete waters include the surface waters of the subarctic gyre and Station 4 where the spring bloom has yet to utilize the majority of the available nutrients after winter mixing.

Within the subarctic gyre, at the time of sampling in the early summer, the remnant winter mixed layer at 100 m water depth could be distinguished from the surface mixed layer above (and sampled at 10 m water depth). The reduction in the nutrient concentrations between 10 and 100 m thus reflects the nutrient utilization at the start of the spring bloom (see Table 1). The relative decrease in nutrient concentrations are 12% and 5% for Stations 2 and 3, respectively, using either Si or P concentrations, and 15% and 14%, respectively, based on N. Difference estimated for N may reflect growth of organisms with preferential uptake of nitrogen at the start of the productive season. The higher nutrient depletion and hence nutrient utilization at Station 2 compared to the more northerly Station 3 is accompanied with warmer less saline surface waters at Station 2, and slightly higher δ^{30}Si values for the surface waters. The Si depletion and Si utilization has resulted in a change of the dissolved δ^{30}Si values by 0.14‰ and 0.09‰, at Stations 2 and 3, respectively. The agreement between the observed and calculated fractionation is excellent given the relatively large errors on such small changes in δ^{30}Si. Unfortunately, at Station 4 the dynamic mixing in the surface waters, as indicated by the salinity and oxygen

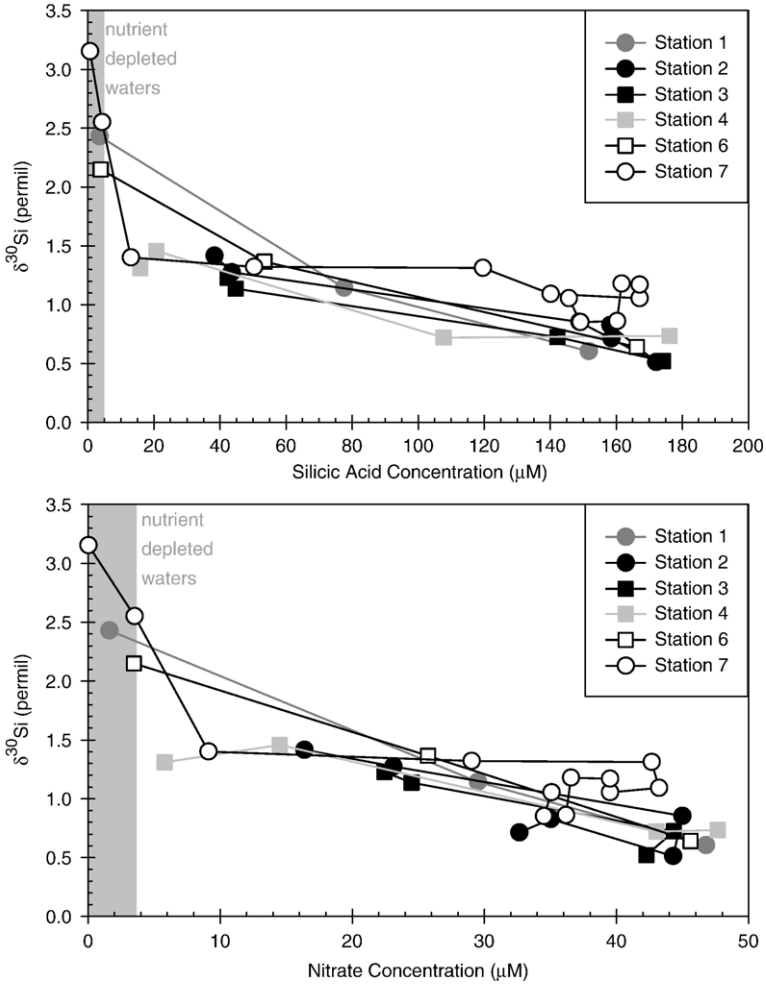

Fig. 4. Seawater δ^{30}Si plotted against [Si] and [phosphate] (in μM) for all North Pacific data. Symbols: gray circles = Station 1, black circles = Station 2, black squares = Station 3, gray squares = Station 4, black open squares = Station 6, and black open circles = Station 7. The gray region denotes low nutrient concentrations, with [Si] and [phosphate] below 5 and 0.3 μM, respectively.

distribution [17], exclude the possibility of quantifying Si isotope fractionation during utilization at this site. From the winter mixed layer δ^{30}Si values of +1.1‰, the isotope composition of biogenic silica formed over the growth season will evolve from +0.1‰ to higher δ^{30}Si values (assuming $\varepsilon = -1$‰). With complete utilisation the average composition of the biogenic silica would equal the initial seawater composition of +1.1‰. With a seasonal cycle that uses 75% of the available Si, the accumulated δ^{30}Si value of the biogenic silica would be +0.6‰. This average δ^{30}Si value exported as biogenic silica from the surface oceans of the HNLC region would mainly dissolve in the water column over the depth range of 100 to 1200 m (see next section).

For Stations in the subtropical gyre, the surface layer does not reflect a closed-system, as nutrients are continuously mixed into the surface waters where they are fractionated. It is further noted that the modelled distribution of dissolved Si isotopes indicates that highest marine δ^{30}Si values lie within the centre of the subtropical gyres and are generated by the progressive fractionation of Si advected within the surface layer, rather than simply high utilization of upwelling nutrients [16]. The highest measured marine Si isotope composition is from the surface waters of Station 7 in agreement with the modelled isotope distribution. As mentioned above, the estimation for the isotope fractionation factor, ε, is strongly biased by the choice of initial conditions used. If we assume that the surface waters are fed simply by the upwelling of nutrients from below we can use the underlying nutrient conditions as the initial conditions. The results for the highly depleted nutrient waters give estimates for ε in a range from −0.6‰ to −1.3‰, which are in reasonable agreement with previous results [13,14]. The relatively large range of the estimated value of ε reflects the poor assumptions used, including the chosen initial conditions, which do not accounted for the dynamic horizontal mixing of the oceans.

4.3. Intermediate waters

On an annual timescale, the surface oceans should be in some sort of steady-state, with the nutrients entrained into the surface waters being matched by the export of organic matter out of the surface oceans. Thus, the average Si isotope composition of sinking biogenic opal from the surface layer, contributes strongly to the Si isotope composition of sub-thermocline waters. For all stations, the increasing Si concentration in the depth between 300 and 1500 m comes directly from the dissolution of biogenic opal sinking through the water column. It should thus be possible to use the change in δ^{30}Si values over this depth range to estimate the average isotopic composition of the biogenic opal that is dissolving into the water column. However, this reasoning misses the dynamics of the system with significant mixing and advection of water masses redistributing silicic acid, and is simply invalid. Horizontal δ^{30}Si gradients not only reflect the composition of biogenic opal dissolving in the water column but also the horizontal mixing of nutrients in the North Pacific, with lower δ^{30}Si values observed in these intermediate depths at more northerly stations, and relatively high δ^{30}Si values in NIPW. The high Si isotope composition of NIPW may be partially due to the Si isotope composition of the source waters, which include thermocline waters with elevated δ^{30}Si values from prior Si utilization.

4.4. Deep water mixing

The differences in the Si isotope composition of deep-water samples can be seen in a plot of δ^{30}Si versus 1/[Si], where mixing between endmember compositions define linear arrays, as shown in Fig. 5. There appears to be two distinct deep-water endmembers with high Si concentrations (low 1/[Si]); one characterized by high δ^{30}Si values (+1.1‰) and the other by slightly lower δ^{30}Si values (+0.5‰). The higher δ^{30}Si endmember reflects water from the deepest samples of Station 7 that is bathed in Lower Circumpolar Water (LCPW) [20], also known as Antarctic Bottom Water (AABW). The lower δ^{30}Si endmember reflects water from depths of 1200 to 1500 m within the western subarctic gyre (WSG), where the highest seawater Si

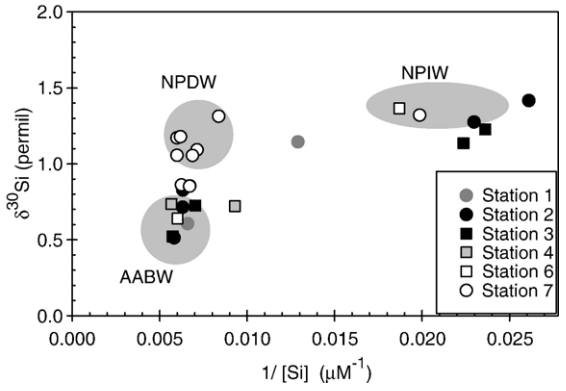

Fig. 5. Seawater δ^{30}Si plotted against 1/[Si(OH)$_4$], for all waters with [Si]>1 ppm, (or 36 μM). Symbols: gray circles = Station 1, black circles = Station 2, black squares = Station 3, gray squares = Station 4, black open squares = Station 6, and black open circles = Station 7.

concentrations characterise North Pacific Deep Water (NPDW) [20]. Vertical eddy diffusivity mixes nutrients from the deep Pacific to more intermediate water depths [26], and can readily explain the mixing between the two deep water endmembers in the Pacific (AABW and NPDW).

The slightly higher δ^{30}Si values of the bottom water compared to NPDW likely reflect the addition of heavy Si isotopes dissolved into this water mass as it flowed under the subtropical gyres. As evident by the surface water composition at Station 7, diatoms growing in the surface waters of the subtropical gyres have δ^{30}Si values as high as +2.4‰ and thus dissolution in the deep sea leads to heavy Si isotope compositions.

Data with low Si concentrations (high 1/[Si]) are from shallower waters, either NPIW or surface waters in the subarctic gyre. The linear array for all data from Stations 2 and 3 from the subarctic gyre define a mixing line between thermocline waters and the average sinking biogenic opal dissolving in the water column, and enriching the deep waters. The intercept of a linear regression indicate that the biogenic silica which is added to the deep waters has an average composition of +0.5‰ and +0.4‰ for Stations 2 and 3, respectively, which is ~0.7‰ lower than the winter surface layer Si isotope compositions. This 0.7‰ difference corresponds to an average annual Si utilization of about 70% of the winter mixed layer for both stations, assuming a closed system and $\varepsilon = 1$‰. A times series of Si concentrations over a yearly cycle from station 2 shows a comparable level of Si utilization, with Si concentrations from >30 μM in winter to <10 μM in summer [27].

Following Sarmiento et al. [23], using the distribution of Si* (defined as [Si] − [NO_3]) in the North Pacific a plume of high Si* is seen north of 30°N in the depth range of 500 to 2000 m (Fig. 6), which corresponds to NPDW. This tracer is an indicator of the nutrient status related to the requirements of diatoms (1:1). Waters from the Southern Ocean, another HNLC region with high diatom production, has Si* values decreasing from positive to negative values across the Polar Front, due to the preferential removal of silicic acid compared to nitrate attributed to diatom growth under iron limiting conditions [23,28]. The strong contrast in the relative nutrient concentrations in the depth range of 100 to 2000 m in the WSG indicates both poor mixing and a separation of the nutrient dynamics, with both N and P being regenerated at much shallower depths below the halocline than Si (Fig. 2). Given that diatoms dominate the planktonic community, this difference may be due to fast regeneration of intracellular nutrients and slow dissolution of siliceous frustules. The slower dissolution of sinking biogenic silica leads to elevated Si* at depth, and may be slower at high latitudes due to cooler temperatures. Mixing of nutrients into the surface waters must have reduced Si:N ratios with the elevated nitrate concentrations, which leads to greater Si limitation during the diatom spring bloom. The very presence of a permanent halocline significantly restricts upwelling to nutrients into the surface layer. The high concentrations of available macronutrients in the late summer indicate that Fe limitation occurs throughout the WSG, and whilst dust dissolution may supply some Fe to the water column, surface water concentrations by late summer are still controlled by Fe limiting conditions [29]. Whatever the limitation of diatom production, the concentrations of Si establish that Si utilization is incomplete and thus Si isotope fractionation restricted. It would thus appear that the low δ^{30}Si values and high Si* of NPDW reflect the strong stratification of the WSG

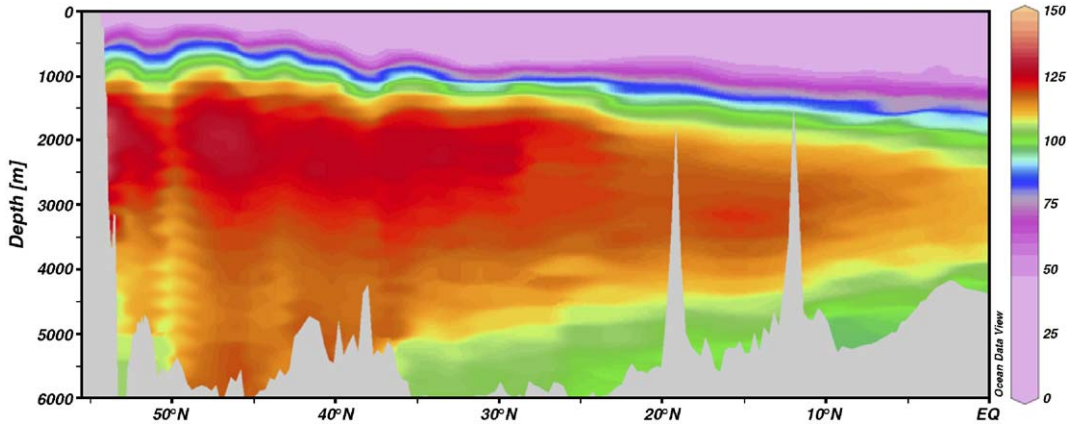

Fig. 6. Distribution of Si* (defined as [$Si(OH)_4$] − [Nitrate]) in a North–South Profile of the western North Pacific along 165°E (data from WOCE transect P13 [43]).

with very limited nutrient mixing into the surface layer and with Fe limitation controlling the utilisation of available silicic acid for diatom growth [4,27].

4.5. Effect of dust dissolution

The eastern part of the North Pacific receives high dust deposition [30], and it might be argued that dust dissolution causes the elevated Si concentrations and high Si* values observed for NPDW. Eolian material would have suitably low δ^{30}Si values as minerals and clays tend to have δ^{30}Si values around or below zero [31]. A 1–10% dissolution of the dust deposition in the NW Pacific (~5 g/m^2/yr [30]) would supply ~1–10 mmol/m^2/yr Si to the water column. Such a small flux is negligible compared to a surface water productivity in the subarctic Pacific of 0.5–5 mol/m^2/yr Si (based on 4–40 mol /m^2/yr C, [32,33] with a Si/C ratio of 0.13 [34]), or an average dissolution in the deep-sea of 0.5 mol/m^2/yr Si [3,35]. Whilst average productivity within the subarctic regions could be at the lower end of this estimated range [32,36,37], so the role of eolian nutrient supply may also be typically over-estimated [38,39]. It is clear that most of the Si that dissolves in the deep-sea is from biogenic opal, and dust dissolution cannot be a significant source of Si with low δ^{30}Si values. It has recently been argued that the dissolution of clays along the coastal margins maybe an important flux of dissolved ions into seawater effecting isotopic mass balances [38,40]. Such a flux has not been included in estimations of the global Si budget [41], but given that clay dissolution rates are much lower than those of biogenic silica, dissolution of clay should be a comparatively negligible flux compared to biogenic silica dissolution from the same sediments.

5. Conclusion

We have measured a wide range of marine Si isotope compositions from the NW Pacific Ocean using new analytical procedures, which allow for the measurement of small and low concentration samples. The observed δ^{30}Si values display a simple relationship to dissolved nutrient concentrations, but this reflects a combination of Si isotope fractionation in the surface waters and mixing between water masses. The biological utilization of Si in the surface waters by diatom biomineralization is the only significant source of Si isotope fractionation in the open ocean. For the subarctic region with nutrient replete conditions, the start of the spring bloom at the time of sampling allows direct assessment of the in situ Si isotope fractionation factor, ε, using a closed-system model. Results agree with previous estimations that ε is about −1‰. Within the subtropical gyre fractionation in the surface waters does not follow a simple closed Rayleigh distillation curve, as active mixing of waters occurs during fractionation. The modelling of isotope fractionation for surface waters within the subtropical gyre as an open-system is problematic, as initial conditions are not defined. Silicon in these waters come from both surface advection and mixing with underlying waters, particularly during storm events. The high dissolved δ^{30}Si values in the subtropical gyres should lead to the deposition of the highest opaline δ^{30}Si values, under these areas [16], although the total amount of opal deposited will be extremely low. The Si isotope composition of deep waters appears to reflect mixing between two components; AABW with δ^{30}Si of about 0.8‰ and NPDW with slightly lower δ^{30}Si values. These low δ^{30}Si values reflect two processes: (i) only partial utilization of dissolved silicic acid occurs in the surface waters over the summer months when diatom growth is ultimately limited by Fe availability even under conditions of high dust deposition and (ii) the nutrient source to the surface waters is dominated by deep waters rather than NPIW which occurs at lower latitudes, and results in the isolation of the nutrient recycling within the subarctic North Pacific.

Acknowledgements

We would like to thank two anonymous reviewers, as well as comments and editorial advice from Harry Elderfield. This work was supported by a grant within the T.M.R. network program STOPFEN of the E.U. to BCR.

References

[1] A.L. Alldredge, C. Gotschalk, U. Passow, U. Riebesell, Mass aggregation of diatom blooms — insights from a mesocosm study, Deep-Sea Res., Part 2, Top. Stud. Oceanogr. 42 (1995) 9–27.

[2] G. Sarthou, K.R. Timmermans, S. Blain, P. Treguer, Growth physiology and fate of diatoms in the ocean: a review, J. Sea Res. 53 (2005) 25–42.

[3] D.M. Nelson, P. Treguer, M.A. Brzezinski, A. Leynaert, B. Queguiner, Production and dissolution of biogenic silica in the ocean — revised global estimates, comparison with regional data and relationship to biogenic sedimentation, Glob. Biogeochem. Cycles 9 (1995) 359–372.

[4] P.J. Harrison, P.W. Boyd, D.E. Varela, S. Takeda, Comparison of factors controlling phytoplankton productivity in the NE and NW subarctic Pacific gyres, Prog. Oceanogr. 43 (1999) 205–234.

[5] J.H. Martin, S.E. Fitzwater, Iron-deficiency limits phytoplankton growth in the northeast Pacific subarctic, Nature 331 (1988) 341–343.

[6] A. Tsuda, H. Saito, J. Nishioka, T. Ono, Mesozooplankton responses to iron-fertilization in the western subarctic Pacific (SEEDS2001), Prog. Oceanogr. 64 (2005) 237–251.
[7] P.W. Boyd, P.J. Harrison, B.D. Johnson, The joint global ocean flux study (Canada) in the NE subarctic Pacific, Deep-Sea Res., Part 2, Top. Stud. Oceanogr. 46 (1999) 2345–2350.
[8] I. Koike, H. Ogawa, T. Nagata, R. Fukuda, H. Fukuda, Silicate to nitrate ratio of the upper sub-arctic pacific and the Bering Sea Basin in summer: its implication for phytoplankton dynamics, J. Oceanogr. 57 (2001) 253–260.
[9] F.A. Whitney, D.W. Crawford, T. Yoshimura, The uptake and export of silicon and nitrogen in HNLC waters of the NE Pacific Ocean, Deep-Sea Res., Part 2, Top. Stud. Oceanogr. 52 (2005) 1055–1067.
[10] C.L. De La Rocha, M.A. Brzezinski, M.J. DeNiro, Fractionation of silicon isotopes by marine diatoms during biogenic silica formation, Geochim. Cosmochim. Acta 61 (1997) 5051–5056.
[11] C.L. De La Rocha, M.A. Brzezinski, M.J. DeNiro, A. Shemesh, Silicon-isotope composition of diatoms as an indicator of past oceanic change, Nature 395 (1998) 680–683.
[12] D.E. Varela, C.J. Pride, M.A. Brzezinski, Biological fractionation of silicon isotopes in Southern Ocean surface waters, Glob. Biogeochem. Cycles 18 (2004), doi:10.1029/2003GB002140.
[13] D. Cardinal, L.Y. Alleman, F. Dehairs, N. Savoye, T.W. Trull, L. André, Relevance of silicon isotopes to Si-nutrient utilization and Si-source assessment in Antarctic waters, Glob. Biogeochem. Cycles 19 (2005), doi:10.1029/2004GB002364.
[14] C.L. De La Rocha, M.A. Brzezinski, M.J. DeNiro, A first look at the distribution of the stable isotopes of silicon in natural waters, Geochim. Cosmochim. Acta 64 (2000) 2467–2477.
[15] G.M. Henderson, New oceanic proxies for paleoclimate, Earth Planet. Sci. Lett. 203 (2002) 1–13.
[16] A. Wischmeyer, C.L. DelaRocha, E. Maier-Reimer, D.A. Wolf-Gladrow, Control mechanisms for the oceanic distribution of silicon isotopes, Glob. Biochem. Cycles 17 (2003) 1083.
[17] C.I. Measures, G.A. Cutter, W.M. Landing, R.T. Powell, Hydrographic observations during the 2002 IOC Contaminant Baseline Survey in the western Pacific Ocean, Geochem. Geophys. Geosyst. (in press), doi:10.1029/2005GC000855.
[18] C.S. Wong, R.J. Matear, H.J. Freeland, F.A. Whitney, A.S. Bychkov, WOCE line P1W in the Sea of Okhotsk — 2. CFCs and the formation rate of intermediate water, J. Geophys. Res.-Oceans 103 (1998) 15625–15642.
[19] I. Yasuda, Y. Hiroe, K. Komatsu, K. Kawasaki, T.M. Joyce, F. Bahr, Y. Kawasaki, Hydrographic structure and transport of the Oyashio south of Hokkaido and the formation of North Pacific Intermediate Water, J. Geophys. Res.-Oceans 106 (2001) 6931–6942.
[20] G.C. Johnson, J.M. Toole, Flow of deep and bottom waters in the Pacific at 10-Degrees-N, Deep-Sea Res., Part 1, Oceanogr. Res. Pap. 40 (1993) 371–394.
[21] D.M. Karl, G. Tien, Magic — a sensitive and precise method for measuring dissolved phosphorus in aquatic environments, Limnol. Oceanogr. 37 (1992) 105–116.
[22] M.A. Brzezinski, J.L. Jones, K.D. Bidle, F. Azam, The balance between silica production and silica dissolution in the sea: insights from Monterey Bay, California, applied to the global data set, Limnol. Oceanogr. 48 (2003) 1846–1854.
[23] J.L. Sarmiento, N. Gruber, M.A. Brzezinski, J.P. Dunne, High-latitude controls of thermocline nutrients and low latitude biological productivity, Nature 427 (2004) 56–60.
[24] R.B. Georg, B.C. Reynolds, A.N. Halliday, (submitted for publication) New sample preparation techniques for determination of Si isotope composition using MC-ICP-MS, Chem. Geol.
[25] B.C. Reynolds, R.B. Georg, M. Frank, A.N. Halliday, Re-assessment of silicon isotope reference materials using high-resolution multi-collector ICP-MS, J. Anal. At. Spectrom. (2006), doi:10.1039/515908.
[26] S. Tsunogai, The western North Pacific playing a key role in global biogeochemical fluxes, J. Oceanogr. 58 (2002) 245–257.
[27] P.J. Harrison, F.A. Whitney, A. Tsuda, H. Saito, K. Tadokoro, Nutrient and plankton dynamics in the NE and NW gyres of the subarctic Pacific Ocean, J. Oceanogr. 60 (2004) 93–117.
[28] V.M. Franck, M.A. Brzezinski, K.H. Coale, D.M. Nelson, Iron and silicic acid concentrations regulate Si uptake north and south of the Polar Frontal Zone in the Pacific Sector of the Southern Ocean, Deep-Sea Res., Part 2, Top. Stud. Oceanogr. 47 (2000) 3315–3338.
[29] M.T. Brown, W.M. Landing, C.I. Measures, Dissolved and particulate Fe in the western and central North Pacific: results from the 2002 IOC cruise, Geochem. Geophys. Geosyst. 6 (2005), doi:10.1029/2004GC000893.
[30] R.A. Duce, P.S. Liss, J.T. Merrill, E.L. Atlas, P. Buat-Menard, B.B. Hicks, J.M. Miller, J.M. Prospero, R. Arimoto, T.M. Church, W. Ellis, J.N. Galloway, L. Hansen, T.D. Jickells, A.H. Knap, K.H. Reinhardt, B. Schneider, A. Soudine, J.J. Tokos, S. Tsunogai, R. Wollast, M. Zhou, The atmospheric input of trace species of the world ocean, Glob. Biogeochem. Cycles 5 (1991) 159–259.
[31] C.B. Douthitt, The geochemistry of the stable isotopes of silicon, Geochim. Cosmochim. Acta 46 (1982) 1449–1458.
[32] L.A. Comeau, A.F. Vezina, M. Bourgeois, S.K. Juniper, Relationship between phytoplankton production and the physical structure of the water column near Cobb Seamount, northeast Pacific, Deep Sea Res., Part 1, Oceanogr. Res. Pap. 42 (1995) 993–1005.
[33] B.C. Booth, Size classes and major taxonomic groups of phytoplankton at 2 locations in the Subarctic Pacific-Ocean in May and August, 1984, Mar. Biol. 97 (1988) 275–286.
[34] M.A. Brzezinski, The Si–C–N ratio of marine diatoms — interspecific variability and the effect of some environmental variables, J. Phycol. 21 (1985) 347–357.
[35] A. Lerman, D. Lal, Regeneration rates in ocean, Am. J. Sci. 277 (1977) 238–258.
[36] D. McDonald, T.F. Pedersen, J. Crusius, Multiple late Quaternary episodes of exceptional diatom production in the Gulf of Alaska, Deep-Sea Res., Part 2, Top. Stud. Oceanogr. 46 (1999) 2993–3017.
[37] S. Banahan, J.J. Goering, The production of biogenic silica and its accumulation on the Southeastern Bering Sea Shelf, Cont. Shelf Res. 5 (1986) 199–213.
[38] T. van de Flierdt, M. Frank, D.-C. Lee, A.N. Halliday, B.C. Reynolds, J.R. Hein, New constraints on the sources and behavior of neodymium and hafnium in seawater from Pacific Ocean ferromanganese crusts, Geochim. Cosmochim. Acta 68 (2004) 3827–3843.
[39] C.I. Measures, M.T. Brown, S. Vink, Dust deposition to the surface waters of the western and central North Pacific inferred from surface water dissolved aluminum concentrations, Geochem. Geophys. Geosyst. 6 (2005), doi:10.1029/2005GC000922.
[40] F. Lacan, C. Jeandel, Tracing Papua New Guinea imprint on the central Equatorial Pacific Ocean using neodymium isotopic

compositions and Rare Earth Element patterns, Earth Planet. Sci. Lett. 186 (2001) 497–512.
[41] P. Treguer, D.M. Nelson, A.J. Vanbennekom, D.J. Demaster, A. Leynaert, B. Queguiner, The silica balance in the world ocean — a reestimate, Science 268 (1995) 375–379.
[42] M.E. Conkright, R.A. Locarnini, H.E. Garcia, T.D. O'Brien, T.P. Boyer, C. Stephens, J.I. Antonov, World Ocean Atlas 2001: Objective Analyses, Data Statistics, and Figures, CD-ROM Documentation, p. 17, National Oceanographic Data Center, Silver Spring, MD, 2002.
[43] R. Schlitzer, Ocean-Data-View, http://www.awi.bremerhaven.de/GPH/ODV, 1999.